CrystEngComm

Cite this: *CrystEngComm*, 2012, **14**, 5845–5853

www.rsc.org/crystengcomm

PAPER

Exploring the structural landscape of 2-aminopyrazines *via* co-crystallizations†

Christer B. Aakeröy,* Prashant D. Chopade, Claudia Ganser, Arbin Rajbanshi and John Desper

Received 6th April 2012, Accepted 28th May 2012
DOI: 10.1039/c2ce25516b

A correlation between the electrostatic charge on the hydrogen-bond acceptor sites of 2-aminopyrazine derivatives and the ability of the compound to form intermolecular hydrogen bonds with carboxylic acids in the solid state has been established. The charge on the hydrogen-bond acceptor can be modulated which leads to a predictable lowering of the supramolecular yield of the reaction. The outcome of all reactions was screened using IR spectroscopy, and twelve new crystal structures are reported to verify the spectroscopic assignments, and to examine the exact nature of the primary intermolecular interactions. The binding preference of carboxylic acids towards the two possible binding sites of 2-aminopyrazines has also been examined, and the main driving force for the assembly of the heteromer between bases and carboxylic acids is the two-point O–H···N/O···H–N synthon. However, seven out of twelve times carboxylic acids also bind *via* a single-point O–H···N synthons. This 'synthon crossover' is unavoidable due to highly competitive binding sites present in the N-heterocyclic bases chosen.

Introduction

Supramolecular chemistry is founded upon reversible non-covalent interactions that are capable of error correction through thermodynamic equilibration. Supramolecular synthesis can, under ideal circumstances, be performed with a minimum amount of effort by using modular subunits encoded with specific functional groups that produce pre-determined architectures through robust and directional molecular recognition events.[1] Supramolecular synthons[2] are kinetically defined structural units that represent the essence of crystals in terms of molecular recognition. A fully rational design of specific molecular solid-state architectures requires a detailed understanding of synthons, but even so, crystal engineering[3] is always likely to offer formidable challenges arising from the use of reversible interactions and the inherent limitations in one-pot reactions.

In the late 1980's, Etter and co-workers systematically employed co-crystallization reactions for probing binding preferences and patterns of functional-group recognition,[4] and this approach still offers arguably the best experimental method for ranking the relative importance of intermolecular interactions.[5] In addition, co-crystals have recently attracted considerable interest as they provide opportunities for changing physical properties of active pharmaceutical ingredients (APIs),[6] and other high-value chemicals[7] without altering molecular structure.[8]

Although many non-covalent interactions are used in co-crystal synthesis ranging from weak π–π interactions[9] to recently emerging halogen bonds,[10] hydrogen bonding[11] remains the primary synthetic tool in this area. Our working strategy for the synthesis of binary co-crystals is based on controlling the affinity between different molecules bearing complementary hydrogen-bonding moieties, thereby manipulating the balance between homomeric and heteromeric interactions (Scheme 1).[12] As part of this strategy, we first need to map out the structural landscape that surrounds interactions between a wide range of molecules bearing a multitude of functional groups.[13]

We have recently shown how hydrogen bonds and halogen bonds can be used side-by-side without synthon crossover as long as the primary molecular recognition events are designed

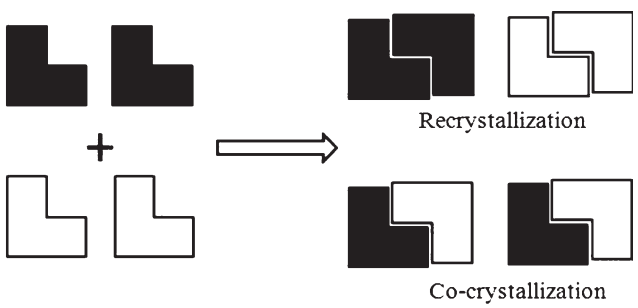

Scheme 1 Recrystallization (top) yields homomeric solids. The co-crystallization process (bottom) leads to a heteromeric product.

Department of Chemistry, Kansas State University, Manhattan, KS, 66506, USA. E-mail: aakeroy@ksu.edu

† Electronic supplementary information (ESI) available: Details of the crystallographic work and cif files. CCDC reference numbers 876776–876787. For ESI and crystallographic data in CIF or other electronic format see DOI: 10.1039/c2ce25516b

around a careful combination of geometric and electrostatic complementarity.[14]

In order to develop versatile supramolecular synthetic strategies based on HB (hydrogen bond) driven self assembly, it is necessary to identify building blocks that display reliable binding preferences in the presence of a range of chemical functionalities. In this study, we have designed ditopic molecules (with two different HB acceptor sites) to test the binding preferences in order to identify a ranking of synthons within an intermolecularly competitive framework. Our choice of building block is guided by a survey of the CSD,[15] which plays a vital part in providing structural information for pattern identification. A search of carboxylic acids with 2-aminopyridine fragments yielded 60 hits and a combination of carboxylic acids with pyridine produced 644 hits (Scheme 2).[16] This shows that carboxylic acids can bind effectively to either moiety through a combination of O–H···N/O···H–N or O–H···N/O···H–C synthons, respectively. To establish the relative strength (and, in effect, supramolecular selectivity) of these two moieties we decided to carry out systematic co-crystallization studies on a probe molecule containing both types of acceptor sites with a series of carboxylic acids. A potential complication with a py/2-NH_2-py competition would result from the fact that most CSD hits corresponding to 2-aminopyridine and carboxylic acids resulted in salts (49 of 60) which would make the comparison flawed. Therefore we needed a backbone containing two sites (in terms of their relative strengths) that are comparable to the pyridine-based system.

Our test system of choice is 2-aminopyrazine as it contains the 2-NH_2-pyrazine moiety and a second "open" heterocyclic nitrogen atom on the same backbone. Importantly, this is a significantly weaker base which should reduce the proclivity for salt-formation compared to that displayed by 2-NH_2-pyridine. In addition, we also wanted to explore the role that electrostatic charge has on the efficiency of the co-crystal synthesis; as most hydrogen bonds are primarily electrostatic in nature, a diminished charge on a hydrogen-bond acceptor is expected to reduce the success rate of co-crystal formation. We opted for three test molecules in this study, Scheme 3, all of which have two main binding sites, and the charge is reduced on the nitrogen atoms through subsequent additions of one and two electron withdrawing substituents, respectively.

A collection of postulated homo- and hetero synthons resulting from reactions between **B1–B3** and a carboxylic acid is shown in Scheme 4.

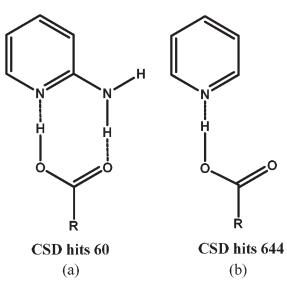

Scheme 2 CSD structural analysis results for synthons under investigation.

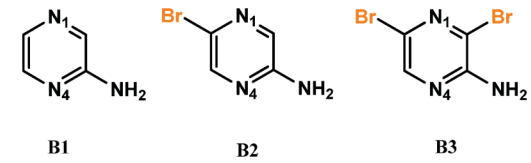

Scheme 3 Ditopic supramolecular reagents for probing selectivity.

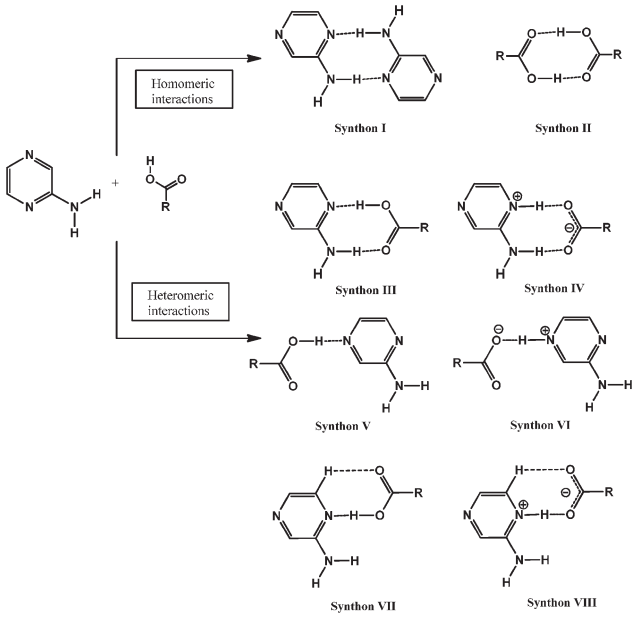

Scheme 4 Potential homo- and hetero synthons in salts and co-crystals of 2-aminopyrazine and a carboxylic acid.

Methodology

Three ditopic supramolecular reagents (Scheme 3, **B1–B3**) were combined with thirty carboxylic acids to establish (i) binding preferences and (ii) supramolecular yield. The bromine substituents alter the charge on the *endo*-cyclic nitrogen atoms, N(1) and N(4), and the electrostatic surface potential for each compound was obtained using semi-empirical PM3 calculations. Co-crystallizations were carried out using 'solvent assisted grinding'[17] (methanol as a solvent[18]) on a mixture of bases and carboxylic acids and the solids from all 90 (3 x 30) reactions were characterized by IR spectroscopy to establish if the result was a reaction (co-crystallization or salt formation) or a no reaction (re-crystallization). The outcome is shown in Table 1. If the result of the reaction was a co-crystallization, based on IR, we attempted to grow crystals suitable for single-crystal X-ray diffraction through slow evaporation. A total of 12 crystal structure determinations were carried out.

Experimental section

All carboxylic acids and 2-aminopyrazine were purchased from Aldrich and utilized without further purification methods. The aminopyrazine derivatives **B2–B3** were synthesized according to previously reported methods.[14] To determine melting points we used a Fisher–Johns melting point apparatus. Infrared spectroscopy was carried out on a Nicolet 380 FT-IR. ^{1}H NMR and ^{13}C

Table 1 Select IR bands in all solids resulting from combinations of **A1–A30** and **B1–B3**

	Acids	B1	B2	B3
A1	4-Aminobenzoic acid	—	—	—
A2	4-Hydroxybenzoic acid	1898, 2521	1898, 2521	—
A3	3,5-Dihydroxybenzoic acid	1878, 2607	1878, 2607	—
A4	2,4-Dimethoxybenzoic acid	1865, 2475	1865, 2475	—
A5	3,4-Dihydroxybenzoic acid	1891, 2448	1891, 2448	—
A6	2,3-Dihydroxybenzoic acid	—	—	—
A7	2,5-Dihydroxybenzoic acid	—	1865, 2410	1818, 2481
A8	2,3-Dimethylbenzoic acid	1885, 2400	—	—
A9	2,5-Dimethylbenzoic acid	—	—	—
A10	Benzoic acid	1911, 2441	—	—
A11	4-Nitrobenzoic acid	1881, 2409	—	—
A12	4-Fluorobenozoic acid	1891, 2521	—	—
A13	Pentafluorobenzoic acid	2050, 2400	—	1879, 2407
A14	3,5-Dinitrobenzoic acid	1860, 2687	1871, 2495	1851, 2355
A15	2,4-Dinitrobenzoic acid	2018, 2381	—	—
A16	3-Nitrobenzoic acid	1898, 2428	—	1851, 2481
A17	2-Chloro-6-fluorobenzoic acid	—	—	1865, 2468
A18	2,6-Difluorobenzoic acid	2004, 2614	—	—
A19	3-Fluorobenzoic acid	1891, 2475	1851, 2521	—
A20	4-Cyanobenzoic acid	1879, 2438	1859, 2448	—
A21	Oxalic acid	2006, 2522	1911, 2349	1838, 2427
A22	Malonic acid	1854, 2455	1918, 2528	—
A23	Succinic acid	1920, 2414	—	—
A24	Glutaric acid	1854, 2400	—	—
A25	Adipic acid	1920, 2520	1859, 2545	—
A26	Pimelic acid	1877, 2495	1869, 2413	—
A27	Suberic acid	1881, 2495	—	—
A28	Azelaic acid	1861, 2483	2450, 1850	—
A29	Sebacic acid	1887, 2475	1834, 2518	—
A30	Dodecanedioic acid	1895, 2507	—	—

NMR spectra were recorded using Varian Unity plus 400 MHz spectrometer in $CDCl_3$.

Synthesis of B2 and B3

N-bromosuccinimide (2.4 g, 13.4 mmol) in 100 ml methylene chloride solution was added dropwise to 2-aminopyrazine (1.0 g, 10.6 mmol) dissolved in methylene chloride (200 mL) cooled to 0–5 °C. The reaction mixture was stirred at 0 °C for 2 h. Upon completion, the reaction mixture was quenched with 10% sodium bicarbonate and 10% sodium sulfite solution followed by filtration. The precipitate was washed with water. The filtrate was extracted using methylene chloride and dried over anhydrous magnesium sulfate. Excess solvent was removed through rotary evaporation. Isolation of a residue was carried out through column chromatography on silica with hexane : ethyl acetate (10 : 0→4 : 6) mixture as the eluant. 2-amino-5-bromopyrazine was isolated as a yellowish–white powder and 2-amino-3,5-dibromopyrazine was a white powder and recrystallized from ethyl acetate : hexane. **B2** (2-amino-5-bromopyrazine), (2.70 g, 62%). Mp. 105–107 °C (Lit. Mp. 105–110 °C);[19] ^{1}H NMR (δ_H; 200 MHz, $CDCl_3$): 8.09 (s, 1H), 7.78 (s, 1H), 4.64 (br, 2H). **B3** (2-amino-3,5-dibromopyrazine), (0.76 g, 12%). Mp. 111–113 °C (Lit. Mp. 109–110 °C);[20] ^{1}H NMR (δ_H; 200 MHz, $CDCl_3$): 8.05 (s, 1H), 5.05 (br, 2H).

Synthesis of co-crystals and salts

B1–B3 were subjected to co-crystallization reactions with thirty different carboxylic acids. We used twenty aromatic monocarboxylic acids: 4-aminobenzoic acid **A1**, 4-hydroxybenzoic acid **A2**, 3,5-dihydroxybenzoic acid **A3**, 2,4-dimethoxybenzoic acid **A4**, 3,4-dihydroxybenzoic acid **A5**, 2,3-dihydroxybenzoic acid **A6**, 2,5-dihydroxybenzoic acid **A7**, 2,3-dimethylbenzoic acid **A8**, 2,5-dimethylbenzoic acid **A9**, benzoic acid **A10**, 4-nitrobenzoic acid **A11**, 4-fluorobenozoic acid **A12**, pentafluorobenzoic acid **A13**, 3,5-dinitrobenzoic acid **A14**, 2,4-dinitrobenzoic acid **A15**, 3-nitrobenzoic acid **A16**, 2-chloro-6-fluorobenzoic acid **A17**, 2,6-difluorobenzoic acid **A18**, 3-fluorobenzoic acid **A19**, 4-cyanobenzoic acid **A20** and ten aliphatic dicarboxylic acids: oxalic acid **A21**, malonic acid **A22**, succinic acid **A23**, glutaric acid **A24**, adipic acid **A25**, pimelic acid **A26**, suberic acid **A27**, azelaic acid **A28**, sebacic acid **A29** and dodecanedioic acid **A30**. These acids were chosen in such a way that we could cover a range of aliphatic and aromatic carboxylic acids, both weak and strong, to ensure that the nature of the carboxylic acids does not affect the binding preference. For co-crystallization, stoichiometric amounts of bases **B1–B3** and acids, either 1 : 1 (monoacids, **A1–A20**) or 2 : 1 (diacids, **A21–A30**), were mixed together.

2-Aminopyrazine 4-nitrobenzoic acid (1 : 2), B1·A11. 2-Aminopyrazine (0.020 g, 0.21 mmol) was dissolved in 1 mL of methanol. To this solution was added 4-nitrobenzoic acid (0.035 g, 0.21 mmol) in 3 mL of methanol. The resulting solution was warmed and allowed to stand for slow evaporation at room temperature. Prism-shaped crystals were obtained after 5 days. M.p. 200–202 °C.

2-Aminopyrazinium 3,5-dinitrobenzoate, B1·A14. 2-Aminopyrazine (0.020 g, 0.21 mmol) was dissolved in 1 mL of methanol. To this solution was added 3,5-dinitrobenzoic acid (0.044 g, 0.21 mmol) in 3 mL of methanol. The resulting solution was warmed and allowed to stand for slow evaporation at room

temperature. Block-shaped crystals were obtained after 7 days. M.p. 158–160 °C.

2-Aminopyrazine 3-nitrobenzoic acid (1 : 1), B1·A16. 2-Aminopyrazine (0.020 g, 0.21 mmol) was dissolved in 1 mL of methanol. To this solution was added 3-nitrobenzoic acid (0.035 g, 0.21 mmol) in 3 mL of methanol. The resulting solution was warmed and allowed to stand for slow evaporation at room temperature. Block-shaped crystals were obtained after 5 days. M.p. 134–136 °C.

2-Aminopyrazine succinic acid (1 : 1), B1·A23. 2-Aminopyrazine (0.020 g, 0.21 mmol) was dissolved in 1 mL of methanol. To this solution was added succinic acid (0.006 g, 0.11 mmol) in 3 mL of methanol. The resulting solution was warmed and allowed to stand for slow evaporation at room temperature. Plate-shaped crystals were obtained after 7 days. M.p. 140–142 °C.

2-Aminopyrazine glutaric acid (1 : 1), B1·A24. 2-Aminopyrazine (0.020 g, 0.21 mmol) was dissolved in 1 mL of methanol. To this solution was added glutaric acid (0.013 g, 0.11 mmol) in 3 mL of methanol. The resulting solution was warmed and allowed to stand for slow evaporation at room temperature. Plate-shaped crystals were obtained after 4 days. M.p. 126–128 °C.

2-Aminopyrazine pimelic acid (1 : 1), B1·A26. 2-Aminopyrazine (0.020 g, 0.21 mmol) was dissolved in 1 mL of methanol. To this solution was added pimelic acid (0.016 g, 0.11 mmol) in 3 mL of methanol. The resulting solution was warmed and allowed to stand for slow evaporation at room temperature. Plate-shaped crystals were obtained after 3 days. M.p. 108–110 °C.

2-Aminopyrazine suberic acid (1 : 1), B1·A27. 2-Aminopyrazine (0.020 g, 0.21 mmol) was dissolved in 1 mL of methanol. To this solution was added suberic acid (0.018 g, 0.11 mmol) in 3 mL of methanol. The resulting solution was warmed and allowed to stand for slow evaporation at room temperature. Plate-shaped crystals were obtained after 5 days. M.p. 210–212 °C.

2-Aminopyrazine sebacic acid (1 : 1), B1·A29. 2-Aminopyrazine (0.020 g, 0.21 mmol) was dissolved in 1 mL of methanol. To this solution was added sebacic acid (0.021 g, 0.11 mmol) in 3 mL of methanol. The resulting solution was warmed and allowed to stand for slow evaporation at room temperature. Plate-shaped crystals were obtained after 4 days. M.p. 124–126 °C.

2-Amino-3,5-dibromopyrazine 2,5-dihydroxybenzoic acid (1 : 1), B3·A7. 2-Amino-3,5-dibromopyrazine (0.020 g, 0.08 mmol) was dissolved in 1 mL of methanol. To this solution was added 2,5-dihydroxybenzoic acid (0.012 g, 0.08 mmol) in 3 mL of methanol. The resulting solution was warmed and allowed to stand for slow evaporation at room temperature. Prism-shaped crystals were obtained after 7 days. M.p. 180–182 °C.

2-Amino-3,5-dibromopyrazine pentafluorobenzoic acid (1 : 1), B3·A13. 2-Amino-3,5-dibromopyrazine (0.020 g, 0.08 mmol) was dissolved in 1 mL of ethanol. To this solution was added pentafluorobenzoic acid (0.016 g, 0.08 mmol) in 3 mL of ethanol. The resulting solution was warmed and allowed to stand for slow evaporation at room temperature. Block-shaped crystals were obtained after 4 days. M.p. 98–100 °C.

2-Amino-3,5-dibromopyrazine 3,5-dinitrobenzoic acid (1 : 1), B3·A14. 2-Amino-3,5-dibromopyrazine (0.020 g, 0.08 mmol) was dissolved in 1 mL of ethanol. To this solution was added 3,5-dinitrobenzoic acid (0.016 g, 0.08 mmol) in 3 mL of ethanol. The resulting solution was warmed and allowed to stand for slow evaporation at room temperature. Plate-shaped crystals were obtained after 7 days. M.p. 128–130 °C.

2-Amino-3,5-dibromopyrazine 2,6-difluorobenzoic acid (1 : 1), B3·A18. 2-Amino-3,5-dibromopyrazine (0.020 g, 0.08 mmol) was dissolved in 1 mL of ethanol. To this solution was added 2,6-difluorobenzoic acid (0.012 g, 0.08 mmol) in 3 mL of ethanol. The resulting solution was warmed and allowed to stand for slow evaporation at room temperature. Block-shaped crystals were obtained after 3 days. M.p. 144–146 °C.

Electrostatic charges

To determine the electrostatic charges on the hydrogen-bond donors and acceptors of the molecules (**B1–B3**) we first used semiempirical PM3 calculations to optimize molecular geometries and then probed the MEPS (0.002 e au^{-1} isosurface, from PM3 calculations) with a point charge. Calculated charges are represented in kJ mol^{-1} (Table 2).

X-Ray crystallography

Data sets were collected on Bruker Kappa APEX II system or a SMART APEX II system, at 120 K using APEX2 software. An Oxford Cryostream 700 low-temperature device was used to

Table 2 Charge calculations (PM3) and outcome summary of co-crystallization experiments between pyrazines and carboxylic acids

	B1, 2-aminopyrazine 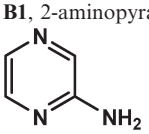		**B2**, 2-amino-5-bromopyrazine 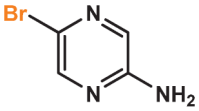		**B3**, 2-amino-3,5-dibromopyrazine 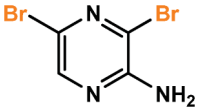	
Charges kJ mol^{-1}	N(1) −251	N(4) −255	N(1) −238	N(4) −245	N(1) −222	N(4) −240
Reaction	25		12		6	
No reaction	5		18		24	
% yield	83		40		20	

Table 3 Crystallographic data for all twelve compounds

	B1·A11	B1·A14	B1·A16	B1·A23	B1·A24	B1·A26	B1·A27	B1·A29	B3·A7	B3·A13	B3·A14	B3·A18
Empirical formula	$C_{18}H_{15}N_5O_8$	$C_{11}H_9N_5O_6$	$C_{18}H_{15}N_5O_8$	$C_{12}H_{16}N_6O_4$	$C_9H_{13}N_3O_4$	$C_{11}H_{17}N_3O_4$	$C_{12}H_{19}N_3O_4$	$C_{14}H_{23}N_3O_4$	$C_{11}H_9Br_2N_3O_4$	$C_{11}H_4Br_2F_5N_3O_2$	$C_{11}H_7Br_2N_5O_6$	$C_{11}H_7Br_2F_2N_3O_2$
Molecular weight	429.35	307.23	429.35	308.31	227.22	255.28	269.30	297.35	407.03	464.99	465.04	411.02
Color, Habit	colourless plate	yellow plate	colourless plate	colourless prism	colourless plate	colourless plate	colourless prism	colourless plate	orange plate	colourless plate	yellow prism	colourless prism
Crystal system	Monoclinic	Triclinic	Monoclinic	Monoclinic	Monoclinic	Monoclinic	Monoclinic	Triclinic	Triclinic	Monoclinic	Triclinic	Monoclinic
Space group, Z	$P2(1)/c$, 2	$P\bar{1}$, 2	$P2(1)/c$, 2	$P2(1)/c$, 2	$P2(1)/c$, 4	$P2(1)/c$, 4	$P2_1$, 2	$P\bar{1}$, 1	$P\bar{1}$, 2	$P2_1/n$, 4	$P\bar{1}$, 2	$P2_1/c$, 4
a/Å	13.8994(7)	7.6755(11)	5.9930(10)	5.3982(9)	5.2487(3)	5.0231(5)	7.7749(5)	5.7935(6)	6.8754(7)	15.5511(6)	7.3153(3)	5.6663(5)
b/Å	5.4845(3)	8.8822(11)	12.1894(18)	19.505(3)	29.2633(18)	34.308(3)	9.8014(7)	7.5090(8)	7.1197(7)	5.8057(2)	10.4607(4)	13.2299(11)
c/Å	13.1317(6)	9.6107(15)	12.995(2)	6.9524(12)	7.2357(5)	7.4377(8)	9.2097(6)	8.7271(8)	13.8665(14)	16.0859(6)	10.8371(4)	17.3426(14)
α (°)	90.00	84.645(10)	90.00	90.00	90.00	90.00	90.00	92.984(4)	87.951(3)	90.00	65.094(2)	90.00
β (°)	101.948(2)	82.063(11)	98.803(8)	104.487(10)	104.958(3)	102.850(5)	101.560(3)	91.952(5)	86.435(3)	111.0750(10)	83.688(2)	93.911(4)
γ (°)	90.00	74.877(10)	90.00	90.00	90.00	90.00	90.00	98.570(5)	72.915(4)	90.00	89.742(2)	90.00
Volume/Å^3	979.36(9)	625.34(15)	938.1(3)	708.8(2)	1073.70(12)	1249.6(2)	687.59(8)	374.57(7)	647.46(11)	1355.17(9)	746.80(5)	1297.05(19)
X-ray wavelength	0.71073	0.71073	0.71073	0.71073	0.71073	0.71073	0.71073	0.71073	0.71073	0.71073	0.71073	0.71073
μ/mm^{-1}	0.117	0.136	0.122	0.112	0.112	0.104	0.099	0.097	6.277	6.054	5.470	6.278
Absorption corr	none	none	multi-scan	none	none	none	multi-scan	none	multi-scan	multi-scan	multi-scan	multi-scan
Reflections collected	12 104	7084	8709	12 115	10 113	15 680	8690	9562	6835	24 119	14 478	31 619
independent	3529	7084	3078	2141	3662	4480	2673	2756	6835	4278	4782	4324
observed	1564	3116	2239	1230	2548	3370	1904	2325	5403	3611	4074	3128
Threshold expression	>2σ(I)	>2σ(I)	>2σ(I)	>2σ(I)	>2σ(I)	>2σ(I)	>2σ(I)	>2σ(I)	>2σ(I)	>2σ(I)	>2σ(I)	>2σ(I)
R_1 (observed)	0.0707	0.0989	0.0494	0.1548	0.0449	0.0449	0.0510	0.0454	0.0429	0.0231	0.0262	0.0327
wR_2 (all)	0.2208	0.3508	0.1511	0.2946	0.1366	0.1366	0.1544	0.1366	0.1280	0.0577	0.0716	0.0721
Goodness of Fit	1.055	1.083	1.106	1.486	0.1366	1.041	1.102	1.069	1.038	1.012	1.056	1.033
$\Delta\rho$ max/min	0.203/−0.315	0.618/−0.499	0.401/−0.277	0.736/−0.433	0.421/−0.229	0.421/−0.229	0.253/−0.140	0.495/−0.225	1.123/−1.147	0.507/−0.423	1.020/−0.676	0.704/−0.653

control temperature. Mo-Kα radiation was used. Initial cell constants were found by small widely separated "matrix" runs. Data collection strategies were determined using COSMO. Scan speeds and scan widths were chosen based on scattering power and peak rocking curves. Crystallographic data for all twelve compounds are summarized in Table 3.

Results

The distinction between reaction (salt/co-crystal) and no reaction was made based on the presence/absence of broad stretches near 1850 and 2500 cm^{-1} which are indicative of intermolecular O–H···N(heterocycle) hydrogen bonds and which will only appear in salts and co-crystals, and not in physical mixtures of the two reactants (Fig. 1 and Fig. 2). Based on IR spectroscopy we determined that **B1**, the strongest base of the three, showed an 83% supramolecular yield followed by 40% and 20% yields for base **B2** and **B3**, respectively.

The results from IR spectroscopy were further supported and complemented by subsequent single crystal X-ray diffraction analysis. In this particular case, where our key goal is to map out the structural landscape of 2-aminopyrazine derivatives, structural analysis provided useful insight. We obtained twelve crystal structures. The relevant X-ray data are summarized in Tables S3–S4 (in ESI).†

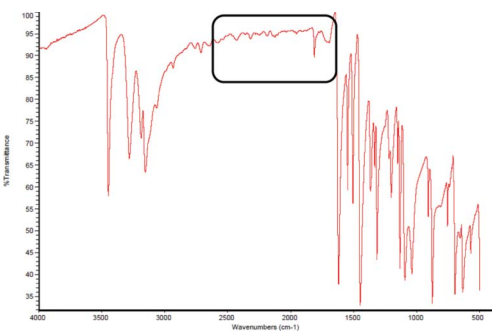

Fig. 1 IR spectrum of attempted co-crystallization of 3,5-dibromo-2-aminopyrazine **B3** and 2,4-dimethoxybenzoic acid (no reaction).

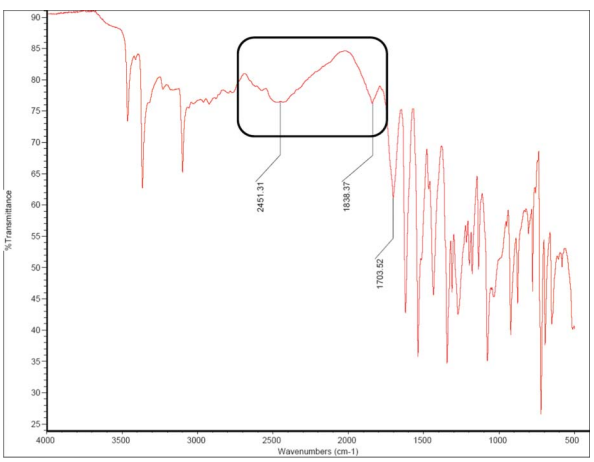

Fig. 2 IR spectrum of successful co-crystallization of 3,5-dibromo-2-aminopyrazine **B3** and pentafluorobenzoic acid.

When **B1** was combined with 3,5-dinitrobenzoic acid **A14**, a 1 : 1 salt was formed (Fig. 3). The primary intermolecular interaction is the charge-assisted two-point N–H···O^-/N^+–H···O^- synthon (Scheme 4, Synthon IV). In addition, the nearest neighbor of the anti-proton of the amino group, is an oxygen atom of a nitro group.

The crystal structure determination of **B1**·**A16** shows 1 : 2 stoichiometry and the expected hydrogen-bond interactions primarily responsible for the supramolecular assembly (Fig. 4a), O–H···N and C=O···H–N (Synthon III and V).

Similarly, the **B1**·**A11** structure showed co-crystal formation (Fig. 4b) *via* previously observed synthon III and V (Scheme 4). Due to the disorder in **B1**·**A11** and **B1**·**A16** it was not possible to establish the secondary interaction of the anti-proton of the amino group.

In the next set, we changed the aromatic acids to aliphatic dicarboxylic acids to test whether changing the nature of the carboxylic acids affects the synthon selectivity. In the structure of **B1**·**A23**, synthon I (Scheme 4) prevailed leaving the carboxylic acid only one option for heteromeric interaction *i.e.* the N(4) binding site of **B1**. The heteromeric synthon observed in co-crystal **B1**·**A23** was O–H···N(4) (Synthon V). To be noted, the potential self-complementary C–H···O hydrogen bond from the C–H of **B1** to the carbonyl of **A23** does not form even though the two molecules are coplanar. The C–H···O distance is 2.875 Å, which is well beyond the van der Waals distance for a hydrogen and oxygen contact, 2.72 Å. The combination of synthon I and heterosynthon V give rise to infinite 1D chains, moreover, these chains are extended into 2D sheets *via* amino anti-NH···O=C secondary interactions (Fig. 5).

When **B1** and glutaric acid **A24** were combined, the outcome was 1 : 1 co-crystal, with the acid binding to both the sites of **B1**.

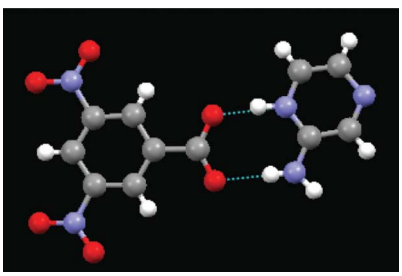

Fig. 3 The primary synthon in the crystal structure of **B1**·**A14**.

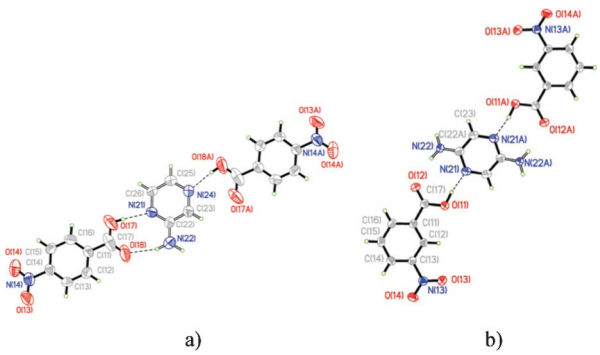

Fig. 4 Thermal ellipsoid plots (50% probability level) of (a) **B1**·**A11** and (b) **B1**·**A16**.

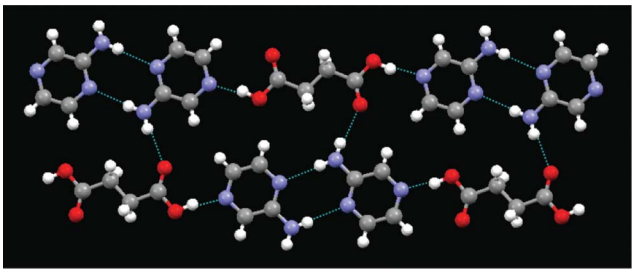

Fig. 5 2D network formed in co-crystal of **B1·A23**.

Synthons III and V (Fig. 6) persisted even when different aliphatic dicarboxylic acids were used (**B1·A26**, **B1·A27**, **B1·A29**).[21] In addition, in all four structures, the anti NH proton interacts with a carbonyl oxygen atom, giving rise to a 2D extended network (Fig. 7).

When **B3** was combined with pentafluorobenzoic acid **A13**, it yielded a 1 : 1 co-crystal with the desired two-point hydrogen bonding synthon I, Scheme 4 (Fig. 8); the same primary synthon was found in the structures of **B1·A7** and **B1·A18**. However, **B3** with 3,5-dinitrobenzoic acid (**A14**) shows an unexpected O–H···N/O···H–C synthon VII, Scheme 5 (Fig. 9). In co-crystals **B3·A13** and **B3·A18**, the anti-proton of the amino group hydrogen bonds to an oxygen atom of a carbonyl group. In the case of **B3·A14**, the anti-proton hydrogen bonds to an oxygen atom of a nitro group of **A14**, whereas in **B3·A7** the anti NH proton is structurally inactive.

Discussion

Controlling supramolecular yield

Based on IR spectroscopy the strongest base of the three, **B1** showed an 83% supramolecular yield followed by 40% and 20% for **B2** and **B3**, respectively. These results can be explained in terms of reduced electrostatic charges on the plausible binding sites of 2-aminopyrazine derivatives due to addition of electron withdrawing substituents, Table 2.

Our systematic analysis also clarifies that heteromeric product formation in this system is primarily determined by the charge on the hydrogen-bond acceptor sites of **B1–B3** and not by the strength of the carboxylic acid (Table S2, ESI†). We analyzed the results in the context of charges of the carboxylic acids (the charge on the acidic proton *i.e.* COO*H*); however, a better correlation was found between the charges on the heterocyclic nitrogen atom and the supramolecular yield. For example, a stronger acid, 2,5-dihydroxybenzoic acid **A7**, gave 'no reaction' with **B1** and **B2**, but a 'reaction' with the weakest base **B3**. This inconsistency of results based on carboxylic acid strengths could

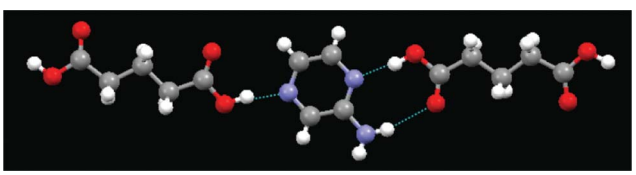

Fig. 6 Infinite 1D chains formed in the co-crystal of **B1·A24**.

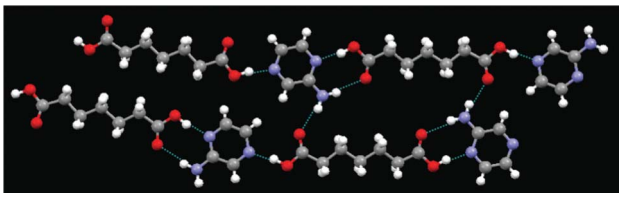

Fig. 7 Extended 2D network formed in the co-crystal of **B1·A26**.

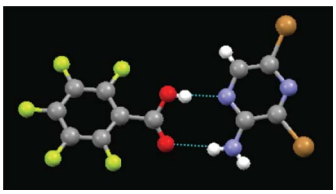

Fig. 8 1 : 1 co-crystal of **B3·A13**.

be due to a prevailing acid–acid dimer even in the presence of N-heterocylic bases.[22]

Synthon classification. In **B1·A11/A16** the carboxylic acid binds to both the ends of **B1**, and in **B1·A14**, where proton transfer from acid to **B1** occurs, it opts for the predicted 2-amino end of **B1**.

The next set of crystal structures we examined were from a combination of **B1** and aliphatic dicarboxylic acids. The observed synthon I (**B1** dimer) in the case of **B1·A23** does not persist upon use of longer chain aliphatic dicarboxylic acids (**B1·A26**, **B1·A26**, **B1·A27**, **B1·A29**). This could be due to prevailing heteromeric interactions over observed homomeric interactions. Also, except **B1·A23**, all remaining four co-crystals from the combination of aliphatic dicarboxylic acids and **B1**, shows remarkable synthon consistency (Table 4). However, selective binding of carboxylic acids at the expected N1 site of **B1** could not be achieved presumably due to the presence of the competitive binding site N4. Although the stronger two-point interaction should prevail over a single-point interaction, but more often for synthon selectivity to occur, geometric and electrostatic factors need to be chosen meticulously.[23]

B3 the weakest of the three bases, yielded four co-crystals **B3·A7**, **B3·A13**, **B3·A14**, **B3·A18**. Three out of four times synthon III was observed and in one exception (**B3·A14**) it showed a never observed synthon VII.[24]

Binding preferences. We investigated the binding preference of carboxylic acids with 2-aminopyrazine derivatives, based on the crystal structures obtained. The structural analysis reveals that ten out of twelve times the carboxylic acids bind, as expected, to the 2-amino end of **B1–B3**. However, in seven out of twelve cases the carboxylic acids bind to N(4) of **B1–B3**.

We performed the CSD analysis for carboxylic acid binding preference when both 2-aminopyridine and pyridine sites are available. The results show that 13 out of 14 times the acid binds to 2-aminopyridine end with one exception where 2-aminopyridine forms a homodimer with the acid binding to a single-point pyridyl nitrogen (Table S4, ESI†). The deviation of the observed results in the 2-aminopyrazine case could be rationalized by examining comparable charges on the two possible binding sites

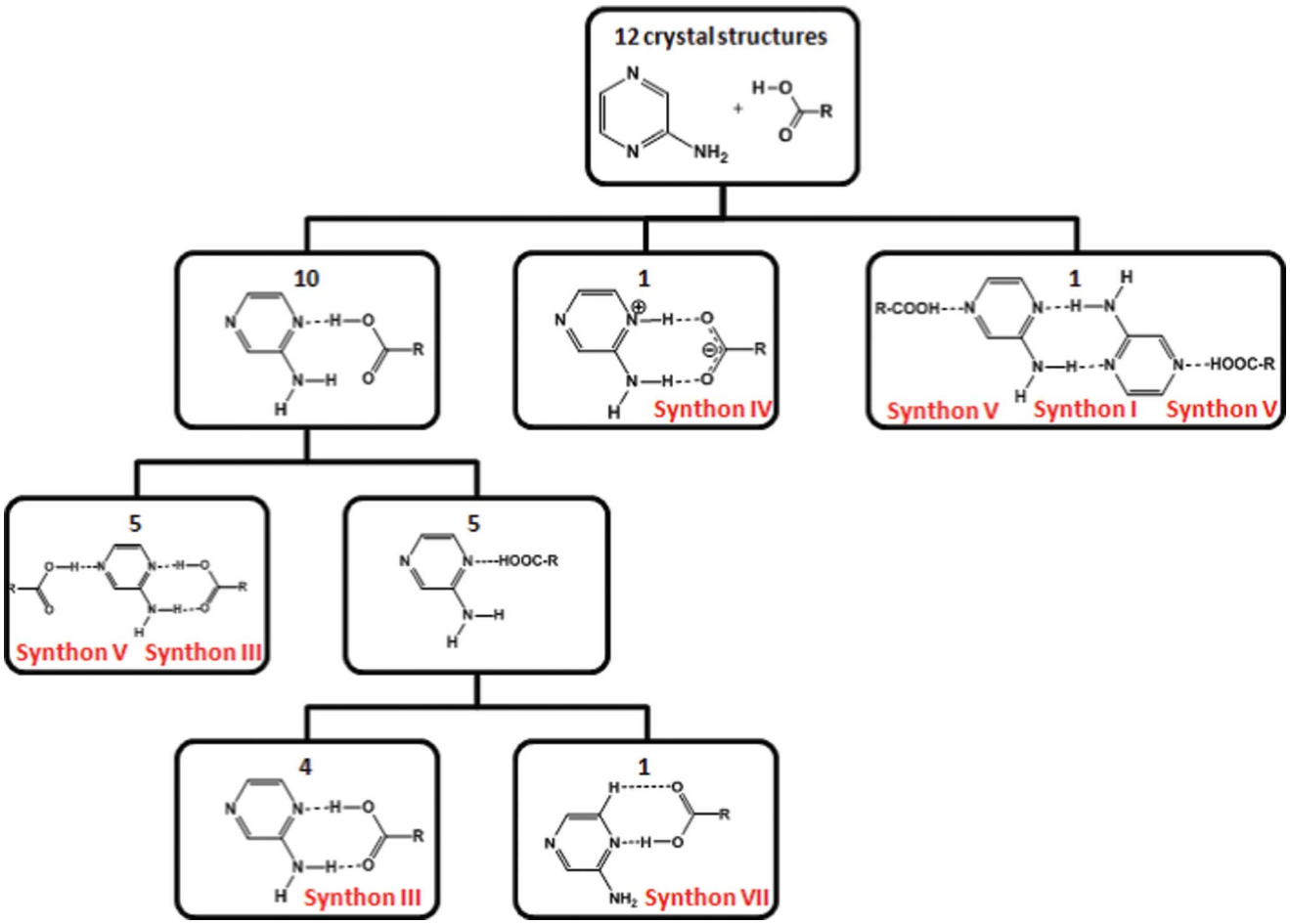

Scheme 5 The structural landscape inhabited by co-crystals of 2-aminopyrazine and carboxylic acids.

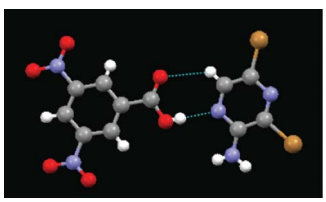

Fig. 9 The primary hydrogen bonds in the crystal structure of **B3·A14**.

Table 4 Summary of observed synthons in crystal structures

	Synthons							
Crystal Structure	I	II	III	IV	V	VI	VII	VIII
B1·A11			✓		✓			
B1·A14				✓				
B1·A16			✓		✓			
B1·A23	✓				✓			
B1·A24			✓		✓			
B1·A26			✓		✓			
B1·A27			✓		✓			
B1·A29			✓		✓			
B3·A7			✓					
B3·A13			✓					
B3·A14							✓	
B3·A18			✓					

(N(1) and N(4) nitrogen atoms) thereby giving more alternatives to carboxylic acids for binding.

Conclusions

Our experimental results successfully establish a relationship between the electrostatic charge on the N-heterocyclic base and the ability of the compound to form intermolecular hydrogen bonds in the solid state. By adding appropriate substituents *via* conventional covalent synthesis, we have been able to modulate the charge on the hydrogen-bond acceptor and this leads to a predictable lowering of the supramolecular yield of the reaction. The main driving force for assembly of a heteromer between bases and carboxylic acids was found to be the O–H···N/O···H–N synthon. However, synthon crossover was observed in the structural landscape of 2-aminopyrazine derivatives combined with carboxylic acids and was unavoidable due to competitive binding sites present in the N-heterocyclic bases chosen. We are currently investigating the role of stoichiometry in controlling the binding ability of carboxylic acids with 2-aminopyrazine derivatives.

Notes and references

1 J.-M. Lehn, *Supramolecular Chemistry: Concepts and Perspectives*, VCH, Weinheim, 1995.

2 G. R. Desiraju, *Angew. Chem., Int. Ed. Engl.*, 1995, **34**, 2311.
3 G. R. Desiraju, *Crystal engineering: The design of organic solids*, Elsevier, Amsterdam, 1989.
4 (*a*) M. C. Etter, *J. Phys. Chem.*, 1991, **95**, 4601; (*b*) M. C. Etter and S. M. Reutzel, *J. Am. Chem. Soc.*, 1991, **113**, 2586; (*c*) M. C. Etter, Z. Urbanczyk-Lipkowska, M. Zia-Ebrahimi and T. W. Panunto, *J. Am. Chem. Soc.*, 1990, **112**, 8415; (*d*) M. C. Etter, *Acc. Chem. Res.*, 1990, **23**, 120.
5 (*a*) C. B. Aakeröy, A. Beatty, M. Nieuwenhuyzen and J. Desper, *Tetrahedron*, 2000, **56**, 6693; (*b*) C. B. Aakeröy, A. M. Beatty and B. A. Helfrich, *J. Am. Chem. Soc.*, 2002, **124**, 14425; (*c*) C. B. Aakeröy, J. Desper and M. E. Fasulo, *CrystEngComm*, 2006, **8**, 586; (*d*) C. B. Aakeröy, J. Desper, D. J. Salmon and M. M. Smith, *Cryst. Growth Des.*, 2006, **6**, 1033–1042; (*e*) C. B. Aakeröy, I. Hussain and J. Desper, *Cryst. Growth Des.*, 2006, **6**, 474–480.
6 (*a*) C. B. Aakeröy, S. Forbes and J. Desper, *J. Am. Chem. Soc.*, 2009, **131**, 17048; (*b*) D. P. McNamara, S. L. Childs, J. Giordano, A. Iarriccio, J. Cassidy, M. S. Shet, R. Mannion, E. O'Donnell and A. Park, *Pharm. Res.*, 2006, **23**, 1888; (*c*) P. Vishweshwar, J. A. McMahon, J. A. Bis and M. J. Zaworotko, *J. Pharm. Sci.*, 2006, **95**, 499.
7 N. Schultheiss, M. Roe and S. X. M. Boerrigter, *CrystEngComm*, 2011, **13**, 611.
8 J. D. Dunitz, *in Perspectives in Supramolecular Chemistry: The Crystal as a Supramolecular Entity*, ed. G.R. Desiraju, Wiley, Amsterdam, 1995.
9 (*a*) N. Barooah, R. J. Sarma and J. B. Baruah, *CrystEngComm*, 2006, **8**, 608; (*b*) N. Motohiro, *CrystEngComm*, 2004, **6**, 130.
10 (*a*) P. Metrangolo, H. Neukirch, T. Pilati and G. Resnati, *Acc. Chem. Res.*, 2005, **38**, 386; (*b*) P. Metrangolo, T. Pilati, G. Resnati and A. Stevenazzi, *Chem. Commun.*, 2004, 1492; (*c*) A. De Santis, A. Forni, R. Liantonio, P. Metrangolo, T. Pilati and G. Resnati, *Chem.–Eur. J.*, 2003, **9**, 3974; (*d*) R. B. Walsh, C. W. Padgett, P. Metrangolo, G. Resnati, T. W. Hanks and W. T. Pennington, *Cryst. Growth Des.*, 2001, **1**, 165; (*e*) D. Cincic, T. Friščić and W. Jones, *J. Am. Chem. Soc.*, 2008, **130**, 7524; (*f*) D. Cincic, T. Friščić and W. Jones, *Chem.–Eur. J.*, 2008, **14**, 747; (*g*) T. Shirman, D. Freeman, Y. D. Posner, I. Feldman, A. Facchetti and M. E. van der Boom, *J. Am. Chem. Soc.*, 2008, **130**, 8162; (*h*) H. L. Nguyen, P. N. Horton, M. B. Hursthouse, A. C. Legon and D. W. Bruce, *J. Am. Chem. Soc.*, 2004, **126**, 1617; (*i*) S. Triguero, R. Llusar, V. Polo and M. Fourmigué, *Cryst. Growth Des.*, 2008, **8**, 2241; (*j*) E. A. Meyer, R. K. Castellano and F. Diederich, *Angew. Chem., Int. Ed.*, 2003, **42**, 1210; (*k*) G. M. Espallargas, L. Brammer and P. Sherwood, *Angew. Chem., Int. Ed.*, 2006, **45**, 435.
11 (*a*) C. B. Aakeröy and D. J. Salmon, *CrystEngComm*, 2005, **7**, 439; (*b*) L. MacGillivray, *CrystEngComm*, 2004, **6**, 77; (*c*) J.-M. Lehn, *Science*, 2002, **295**, 2400; (*d*) G. R. Desiraju, *Acc. Chem. Res.*, 2002, **35**, 565; (*e*) B. Moulton and M. J. Zaworotko, *Chem. Rev.*, 2001, **101**, 1629; (*f*) G. R. Desiraju, *Angew. Chem., Int. Ed. Engl.*, 1995, **34**, 2311; (*g*) M. Wenger and J. Bernstein, *Angew. Chem., Int. Ed.*, 2006, **45**, 7966; (*h*) S. L. Childs and K. I. Hardcastle, *CrystEngComm*, 2007, **9**, 364; (*i*) E. Bosch, *CrystEngComm*, 2007, **9**, 191; (*j*) V. R. Pedireddi, S. Chatterjee, A. Ranganathan and C. N. R. Rao, *J. Am. Chem. Soc.*, 1997, **119**, 10867; (*k*) C. B. Aakeröy, J. Desper and J. F. Urbina, *CrystEngComm*, 2005, **7**, 193; (*l*) C. B. Aakeröy, N. Schultheiss and J. Desper, *J. Mol. Struct.*, 2010, **972**, 35; (*m*) C. B. Aakeröy, J. Desper and B. M. T. Scott, *Chem. Commun.*, 2006, 1445.
12 (*a*) J. A. Bis and M. J. Zaworotko, *Cryst. Growth Des.*, 2005, **5**, 1169; (*b*) K. Merz and V. Vasylyeva, *CrystEngComm*, 2010, **12**, 3989; (*c*) G. R. Desiraju, *J. Mol. Struct.*, 2003, **656**, 5; (*d*) N. R. Goud, N. J. Babu and A. Nangia, *Cryst. Growth Des.*, 2011, **11**, 1930.
13 (*a*) B. Sarma, N. K. Nath, B. R. Bhogala and A. Nangia, *Cryst. Growth Des.*, 2009, **9**, 1546; (*b*) J. A. Bis, P. Vishweshwar, D. Weyna and M. J. Zaworotko, *Mol. Pharmaceutics*, 2007, **4**, 401; (*c*) C. B. Aakeröy, A. M. Beatty and B. A. Helfrich, *Angew. Chem., Int. Ed.*, 2001, **40**, 3240; (*d*) E. Corradi, S. V. Meille, M. T. Messina, P. Metrangolo and G. Resnati, *Angew. Chem., Int. Ed.*, 2000, **39**, 1782.
14 (*a*) C. B. Aakeröy, P. D. Chopade, C. Ganser and J. Desper, *Chem. Commun.*, 2011, **47**, 4688; (*b*) C. B. Aakeröy, P. D. Chopade and J. Desper, *Cryst. Growth Des.*, 2011, **11**, 5333.
15 F. A. Allen, *Acta Crystallogr., Sect. B: Struct. Sci.*, 2002, **58**, 380.
16 CSD search carried out on ConQuest Version 1.12. (Updated till November 2011).
17 S. L. James, C. J. Adams, C. Bolm, D. Braga, P. Collier, T. Friščić, F. Grepioni, K. D. M. Harris, G. Hyett, W. Jones, A. Krebs, J. Mack, L. Maini, A. G. Orpen, I. P. Parkin, W. C. Shearhouse, J. W. Steed and D. C. Waddell, *Chem. Soc. Rev.*, 2012, **41**, 413.
18 We attempted 'solvent assisted grinding' using different solvents and melt experiments for co-crystal screening. However, while using different solvents (*e.g.* dichloromethane, chloroform) for grinding, solubility problem of acids/bases encountered and when melted, the compounds decomposed.
19 R. C. Ellingson and R. L. Henry, *J. Am. Chem. Soc.*, 1949, **71**, 2798.
20 W. W. Paudler and M. V. Jovanovic, *J. Org. Chem.*, 1983, **48**, 1064.
21 Crystal structure **B1·A29** has amino group disordered in 50 : 50 ratio.
22 (*a*) P. L. Wash, E. Maverick, J. Chiefari and D. A. Lightner, *J. Am. Chem. Soc.*, 1997, **119**, 3802; (*b*) C. B. Aakeröy, A. M. Beatty and K. R. Lorimer, *J. Chem. Soc., Dalton Trans.*, 2000, 3869.
23 (*a*) C. B. Aakeröy, J. Desper, B. A. Helfrich, P. Metrangolo, T. Pilati, G. Resnati and A. Stevenazzi, *Chem. Commun.*, 2007, 4236; (*b*) C. B. Aakeröy, N. Schultheiss, A. Rajbanshi, J. Desper and C. Moore, *Cryst. Growth Des.*, 2009, **9**, 432.
24 CSD search shows no hits on this type of synthon in presence of 2-aminopyridine based heterocycles.